Supplemental materials and methods

PET/CT Imaging

PET/CT Scanners

All PET/CT scans were performed in our BSL-3 imaging suite using a hybrid preclinical PET/CT system integrated by our group. The system is comprised of a microPET Focus 220 preclinical PET scanner designed for primate imaging (Siemens Molecular Solutions, Knoxville, TN) and a fully mobile clinical 8-slice helical CT scanner (Neurologica Corp, Danvers, MA) (1). The microPET Focus 220 (F220) consists of four rings of position sensitive scintillation detectors, with each ring consisting of 42 detector blocks. Each detector block is comprised of a 12 x 12 array of Lutetium Oxyorthosilicate (LSO) crystals (1.5 x 1.5 x 10 mm), giving 24,192 individual detector elements. Each element is coupled via optical fibers to a multi-channel photomultiplier tube. The bore opening of the F220 measures 22 cm in diameter with an effective imaging field-of-view (FOV) of ~19 cm radially and 7.6 cm axially. (2) The CereTom CT has a bore opening of 32 cm, and generates up to 8 slices per revolution (1 cm/sec) at an axial collimation of 1.25mm.

The PET and CT scanners are arranged inline as with clinical PET/CT systems. Both PET and CT subsystems are serviced by a custom engineered external bed that replaces the standard microPET bed. Control of this bed is via the integral controller on the microPET scanner that is used to control the factory supplied bed. This arrangement provides intrinsically co-registered CT and PET images acquired sequentially with the subject on a common imaging pallet with an axial co-scan range of greater than 50 cm (the axial extent of the imaging pallet able to be imaged by both PET

and CT). The CereTom CT scanner rests on an aluminum plate and rail system that matches the gantry isocenters and allows fine adjustments to the alignment of the systems. Volume (helical) acquisition is achieved by the movement of the entire CT system axially along a set of rails while the x-ray source is energized and in rotation.

Animal sedation, contrast and [18F] FDG injection:

Animals were fasted for 24 hour prior to PET/CT imaging. Animals were sedated for scanning with ketamine (10-20 mg/kg) with atropine (0.02-0.04 mg/kg) intramuscularly followed by ventilation with isoflurane (0.5-2%) to maintain anesthetic depth and mechanically ventilated (eVent Medical Inspiration LS Ventilator). Approximately 185 MBq of [^{18}F]FDG was injected into each animal via saphenous vein and allowed to distribute for 45 minutes prior to imaging. The animal was then positioned prone on the unified imaging pallet.

PET/CT Image acquisition:

During the FDG uptake period, a CT topogram (scout scan) was acquired and used to identify the axial extent of the area to be imaged. Subsequently, a contrast-enhanced CT scan (9 cc of Iopamidol (Isovue®) 370) was acquired over the target area with the lungs maintained at a fixed pressure of 3 cm H_2O (297 Pa) using the ventilator. For PET acquisition, the bed was automatically moved to position the animal within the PET field-of-view and emission data acquired for 3 - 4 bed positions (10 min per bed position), each covering 8 cm axially with an overlap of 13 mm. The ventilation-breathing protocol was optimized to maximize the duty-cycle dwell time at a positive-end-expiratory-pressure (PEEP) of 3cm H_2O to minimize respiratory motion artifacts in the PET images and optimize registration with the breath-hold CT images.

Image reconstruction:

CT images were reconstructed at the native resolution using the high-resolution sharp-lung filter. A CT-based attenuation correction (CTAC) procedure, using the co-registered CereTom CT appropriately transformed, was used to correct for scatter and absorption of the PET emission data. (This replaces the lengthy lower quality ^{68}Ge/^{68}Ga or ^{57}Co point-source transmission scan that is the standard method of attenuation and scatter correction for the microPET Focus 220. CTAC is a well-validated procedure that is standard on all commercially available PET/CT systems.) PET images were reconstructed using the vendor supplied [OSEM-3D] algorithm on a 256x256 matrix. PET and CT images were registered using the rigid-registration algorithm on the Inveon Research Workstation (Siemens Preclinical Solutions), as there was little deformation between the PET and CT images due to the controlled ventilation employed during the acquisitions.

Data analyses:

High variability in observed SUV motivated the analysis of the data using a SUV ratio (SUVR). Normal liver parenchyma was rejected as a reference due to the liver toxicity of the chemotherapy agents. Instead, resting muscle was chosen which reduced the variability in the longitudinal analysis considerably, which is likely due to a multiplicity of factors, such as the influence of isoflurane, and the reduced availability of FDG in cases with very high cardiac uptake or large active consolidations. One left and one right ROI were propagated through ten PET axial slices at the level of the carina for normal muscle mean FDG uptake. A cylinder muscle mean SUV ratio was used for all PET analyses (glycolytic index, partial volume corrected SUVR of granulomas, lymph node

SUVR and whole-lung PET).

Glycolytic index (G.I. = volume*mean SUV) was computed to analyze consolidations. A volume of interest was generated on the PET image using a region growing algorithm implemented in the OsiriX viewer, an open-source PACS workstation and DICOM image viewer. For this operation, a SUV minimum of four was selected and the resulting region manually edited as necessary with the brush ROI erase tool to exclude adjacent uninfected FDG avid tissue (i.e. heart) and other unrelated pathology. The dilate, close, and erosion brush ROI functions were used to include all lower SUV pixels of the consolidation, guided by CT. Lesion volume (cm^3) and SUV mean were then recorded. Granulomas (N=5-8 per monkey) were randomly selected and tracked in serial scans. Lesion size on CT was measured in the axial view and a ROI (region of interest) was drawn on the PET image in the axial view to measure SUV_{max}. A partial volume correction factor was applied to the SUV_{max} based on spheres of known size and fixed radioactivity concentration. All lymph nodes that were FDG avid were serially analyzed by SUVR.

The whole-lung PET metric was calculated as follows: Regions of aerated lung < 500 Hounsfield units (HU) were identified on CT using a region growing algorithm on the OsiriX viewer with manual selection of seed points. A closing operation was performed to include isolated nodules and diffuse disease. The region was manually transferred to the corresponding co-registered PET image and was merged with any regions of consolidation present (which are identified using region growing of elevated PET signal and manual editing as described previously) to give a whole-lung region of interest. The standard uptake values normalized to the resting muscle signal were summed for all

voxels, and the total for each animal scan was divided by the total for that animal's baseline scan, which is acquired with clear lungs prior to infection.

References:

1. Rumbolt Z, Huda W, All JW. Review of Portable CT with Assessment of a Dedicated Head CT Scanner. American Journal of Neuroradiology. 2009;30:1630-6.
2. Tai YC, Ruangma A, Rowland D, Siegel S, Newport DF, Chow PL, et al. Performance evaluation of the microPET focus: a third-generation microPET scanner dedicated to animal imaging. J Nucl Med. 2005;46(3):455-63.

Supplemental figures
Figure S1

A

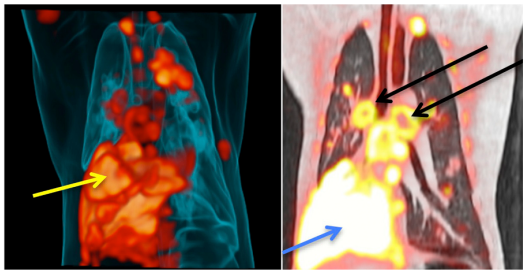

B

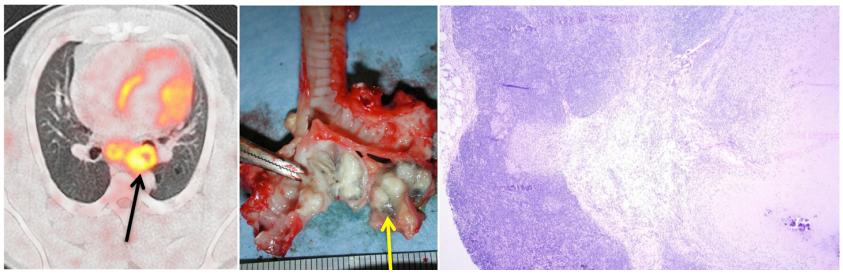

Fig. S1. A) Left panel: A 3-D rendering of tuberculous lung disease by ^{18}F-FDG PET CT with a large right lower lobe consolidation (yellow arrow). Disease is also seen in the left upper lobe. Right panel: Coronal sections of the lung show large, FDG-avid mediastinal lymph nodes with central necrosis (seen as absence of FDG uptake) (black arrows). The large right lower lobe consolidation is also seen (blue arrow). B) Axial view of the right carinal lymph node with lack of FDG uptake in the center of the node is shown suggesting necrosis. Central necrosis was confirmed by gross pathology (yellow arrow in middle panel) with caseum partially effacing normal lymph node structure. Histopathologic evidence of caseous necrosis (right panel) of the same lymph node is seen within adjacent to normal lymph node architecture (left) (right panel, H&E stained, 4x magnification).

Figure S2

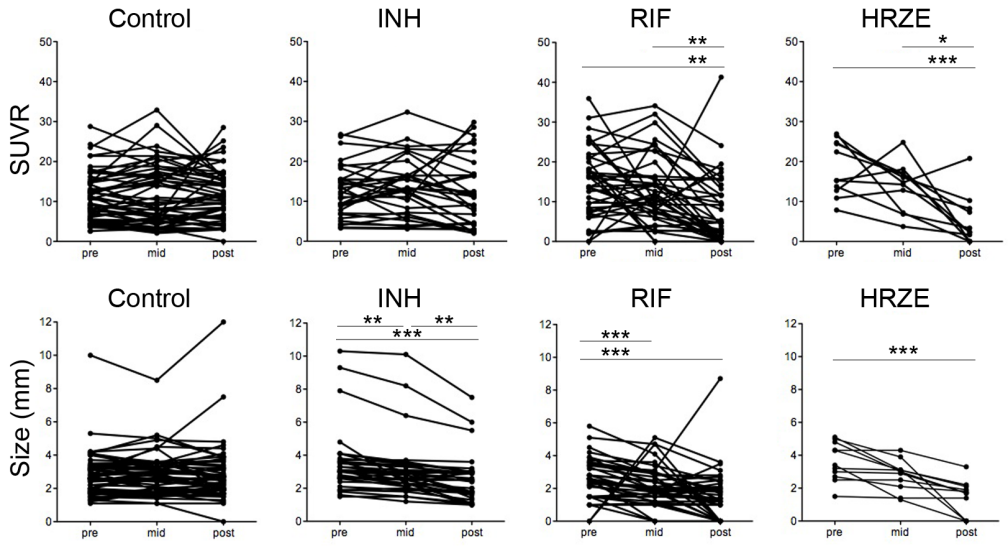

Fig. S2. PET CT changes in lung granulomas by metabolic activity (top row) and size (bottom row) with and without drug treatment taken immediately prior to (pre), middle and (mid) and end of treatment (post). Reductions in metabolic activity (SUV) occur in individual granulomas with RIF and HRZE treatment between pre- and post treatment and between mid and post treatment. INH along, RIF alone and HRZE show reduce granuloma size during treatment. Friedman's test, $p<0.05$, post hoc Dunn's multiple comparison, *$p \leq 0.05$, **$p \leq 0.01$, ***$p \leq 0.001$. Rifampin (RIF), INH (isoniazid), HRZE (isoniazid, rifampin, pyrazinamide, ethambutal).

Figure S3

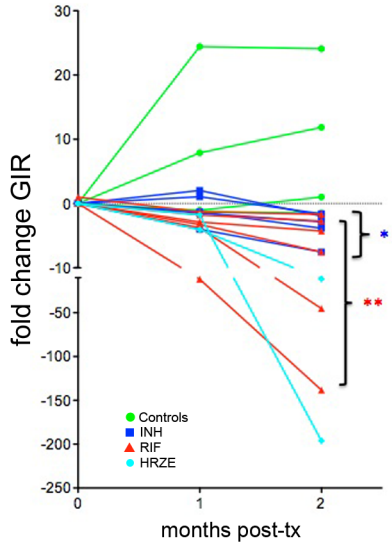

Fig S3. Reduction in metabolic activity within lung consolidations occurs with INH alone and RIF alone treatment. Changes in metabolic activity of lung consolidations are measured by geometric index ratio (GIR) in the y-axis. The x-axis shows the months of treatment. Each line represents an individual animal. Friedman's test $p<0.05$, post hoc Dunn's multiple comparison,*$p \leq 0.05$ (INH group), **$p \leq 0.01$ (rifampin group). Too few data points were available to compare HRZE treatment. Green line= control groups (no treatment) (n=4), dark blue line= isoniazid-treated (n=5), red = rifampin-treated (n=4), and light blue = HRZE-treated (n=2).

Figure S4

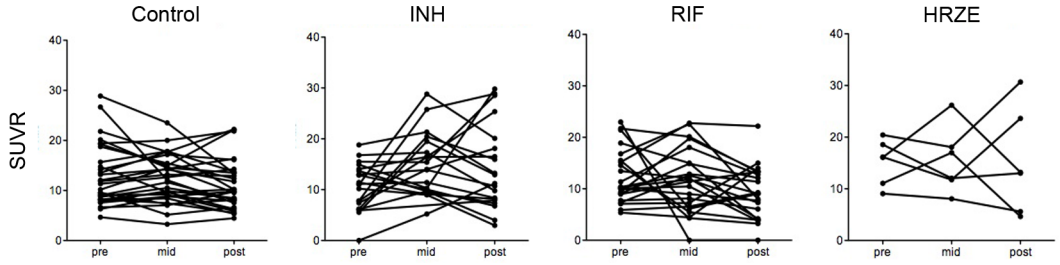

Fig. S4. ^{18}F-FDG PET CT changes (measured as standard uptake unit ratio, SUV) in mediastinal lymph nodes before (pre), at 1 month drug treatment (mid) and 2 months drug treatment (post). Control animals received no drug. Isoniazid= INH, rifampin=RIF, HRZE (isoniazid, rifampin, pyrazinamide, ethambutal).

Figure S5

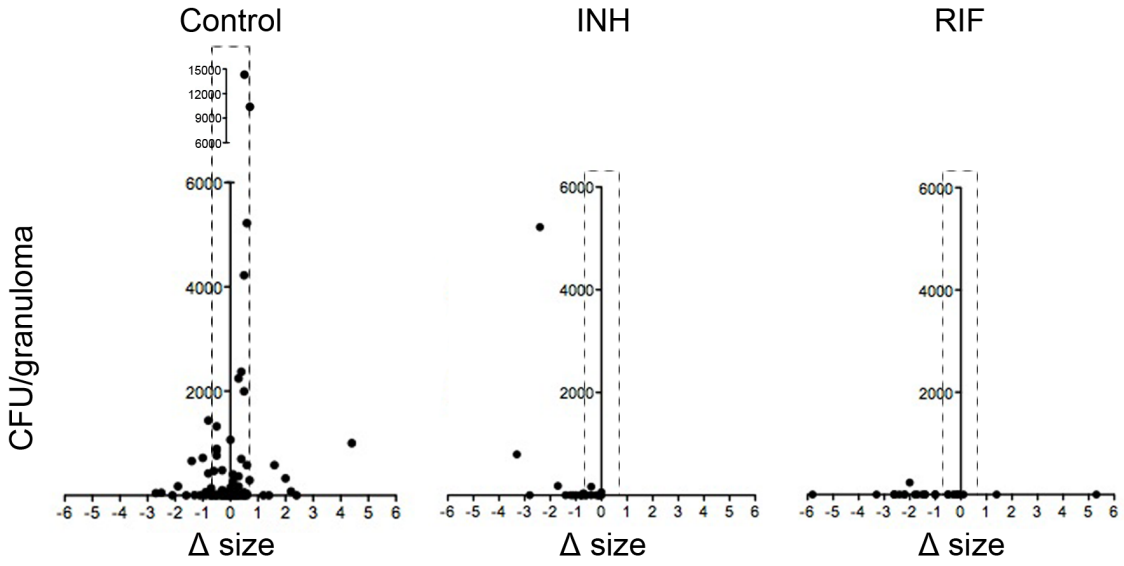

Fig. S5. Distribution of granuloma specific bacterial burden (measured as CFU/gran) and change in granuloma size (delta size) with and without drug treatment. Most granulomas showed reduction in size with drug treatment (INH and RIF) that had low bacterial burden). In contrast, control animals had lesions that increased and decreased in size over time. Bacterial burden within the granuloma was detected in lesions that both increased and decreased in size. Dotted lines reflect the margin of error estimated by the variation in size estimates between CT scans. Isoniazid= INH, rifampin=RIF